# DE NOVO SIMULATION AND SPECTROSCOPIC STUDY OF IRON SPECIATION IN MICRO- AND MESOPOROUS BIOMIMETIC MATERIALS ACTIVE IN THE SELECTIVE OXIDATION OF METHANE

*Peter-Paul H.J.M. Knops-Gerrits*

Département de Chimie, Université Catholique de Louvain (UCL), Batiment LAVOISIER, Place L. Pasteur n°1, B-1348 Louvain-la-Neuve, Belgium

**Introduction**

Methane Mono-Oxygenase (MMO) and Deoxyhemerythrin are examples of diiron enzymes that catalyze the dissociative and non-dissociative binding of molecular oxygen [1-5]. Dissociative binding of oxygen via a peroxo intermediate to a diamond core structure leads to a reactive species active in the oxidation of alkanes [1-2]. Non-dissociative binding of oxygen via a side-on peroxo intermediate such as in the active site of deoxyhemerythrin does not allow the splitting and allows binding/release of oxygen as a function of the physiological conditions. Such active sites are among the growing list related to (hydr)oxo-bridged di- or poly-iron cores in biological systems. Methane mono-oxygenase has a binuclear active site in which two histidines and four glutarates are present. Both iron ions are coordinated by a histidine, an oxygen from a bridging carboxylate and a μ-oxo bridge [1]. Theoretical modeling of these enzyme active sites has been recently reported. Yoshizawa *et al.* studied the dioxygen cleavage and methane activation on diiron enzyme models with the extended Hückel method, an approximate molecular orbital method, the μ-$\eta^1$:$\eta^1$-$O_2$ or μ-$\eta^2$:$\eta^2$-$O_2$ binding modes are distorted to the corresponding dioxygen complex [4].Shestakov and Shilov showed that the synchronous insertion of O atom mechanism is found to be significantly less contradictory (for example in methane) if it is supplemented by the stage of formation of the five-coordinate carbon intermediate complex of a hydrocarbon molecule via oxygen atom of an active center[5].

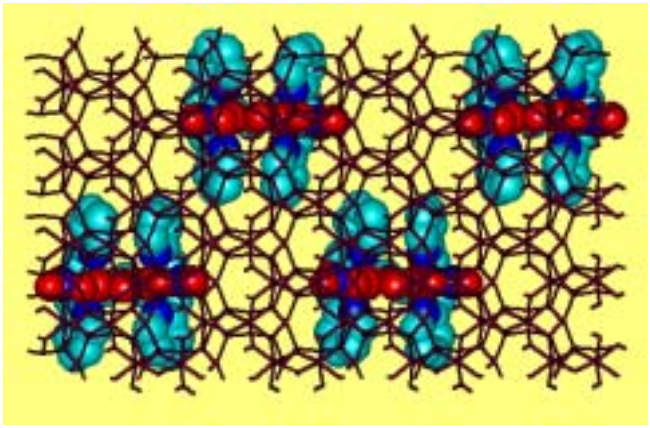

**Figure 1.** [$Fe_2$(HPTP)(OH)$(NO_3)_2$] in montmorillonite clays.

**Methane can be converted into methanol with binuclear iron(IV)-model complexes**

To mimic the MMO active site with a finite cluster we chose to study the binuclear heptapodate coordinated iron (III)-complexes of *N,N,N',N'*-tetrakis(2-benzimidazolylmethyl)-2-hydroxy- 1,3-diamino -propane (HPTB) and *N,N,N',N'*,-Tetrakis(2-pyridylmethyl)-2-hydroxy-1,3-diamino-propane (HPTP). These have active sites of the form [$Fe_2$(HPTP)(μ-OH)]$^{4+}$ (1) and [$Fe_2$(HPTB)(μ-OH)]$^{4+}$ (2). As supports for such complexes we use mesoporous materials such as MCM-41, FSM-16, HMS (Hexagonal Molecular Sieve) [7-8] and clays (Fig 1) [9] since these materials have large surface areas and large pore sizes that can be tuned from 1.5 to 10 nm. We characterized these complexes using Quantum Mechanics (QM) and EXAFS, Mössbauer and Catalysis and studied the effect of the support.

The QM was at the *ab initio* and DFT (B3LYP) levels [3]. All chelating N-atoms and the ligand backbone were included in the QM determination of the geometry and electronic properties of the ground and excited states of the active site. The geometries of the supported complexes were determined with MD using the Universal FF (UFF) [6] supplemented with a FF based on the quantum mechanics. For the $O_2$ binding on the reduced active site the μ-$\eta^1$:$\eta^1$-$O_2$ mode seems to preceed formation of the O=Fe-O-Fe=O bis-ferryl active site that reacts exothermally with methane by 50.56 kcal/mol. After the H splitting from methane, the methyl recombines with the FeO center via a weak Fe-$OCH_3$ bond in this model. The consecutive reaction with water protonates the methoxy group to form methanol and the substitution at the active site by a hydroxo group is endothermic by 7.50 kcal/mol. The regeneration of the active site with $H_2O_2$ is again endothermic by 3.24 kcal/mol. After the loss of methanol $Fe^{(III)}$- O- $Fe^{(III)}$ is formed which is reduced to the Fe(II,II) form. Ferryl groups are reactive two center three electron bonds. The solvation calculations are very important to obtain good quantitative data. Siegbahn *et al.* [1] uses gas-phase values as the dielectric constant of an enzyme is low (ε = 4) compared to this of water (ε = 80). For the solvation of small model compounds in water such effects are not negligable. The solvation energies are about 150, 300 and 500 kcal/mol for the 2+, 3+ and 4+ complexes.

Mössbauer spectroscopy allows the oxidation and spin states of the iron atoms to be assessed. Thus the isomer shifts relative to metallic iron at 300 K in the range 0.35-0.60 mm/s are characteristic of 5- or 6-coordinate high-spin di-ferric μ-OH complexes, the smaller quadrupolar splitting < 1 mm/s, in the hydroxo-bridged complexes is due to the lengthening of the Fe-O bond upon protonation of the oxo bridge. The Mössbauer pattern of the supported complexes becomes more complex due to complex lattice interactions. The EXAFS shows lengthening of the Fe-Fe distances for benzimidazole compared to pyridine containing complexes. When the complexes are supported on mesoporous oxides, the EXAFS finds a lengthening of the Fe-Fe distances. The EXAFS data on the model compounds gives longer Fe-Fe distances than the QM. This may be due to neglecting in the QM the large counterbalancing anions associated with the structure of [$Fe_2$(HPTP)(μ-OH)$(NO_3)_2$]$(ClO_4)_2$ and [$Fe_2$(HPTB)(μ-OH)$(NO_3)_2$]$(ClO_4)_2$.

**Methane can be converted into methanol with α-Oxygen on iron in ZSM5 type zeolites**

α-Oxygen can be formed on such iron sites by nitrous oxide $N_2O$ decomposition at elevated temperature. Nitrous oxides are formed in the industrial synthesis of adipic acid. In nitrous oxide decomposition several routes exist depending on pressure and temperature. In order to study the pretreatment, activation, reaction and extraction effects the Fe containing topologies such as CHA, MFI, MOR and CFI [10] are tested in the methane to methanol conversion. Pretreatment performed with $O_2$ at 550°C and vacuum at 800°C to 900°C is optimal. Activation with $N_2O$ at 250°C is optimal and reaction with $CH_4$ occurs from 20°C, extraction is best with $H_2O$ and quantification of methanol is performed by GC, GC-MS and NMR. Structure/activity effects rquire the notion of new structural parameters related to the introduction of iron in zeolite topologies such as CHA, MFI, MOR and CFI [10-11], performed via direct

# DECOMPOSITION OF $CF_4$ BY MICROWAVE HEATING

*Franz-Josef Spiess and Steven L. Suib*

Department of Chemistry, University of Connecticut,
55 N.Eagleville Rd., Storrs, CT 06268

## Introduction

Carbon tetrafluoride is an inert gas that is also a greenhouse gas with a very high global warming potential. It is a by-product in the aluminum production and used in the semiconductor industry. The exceptionally long atmospheric lifetime of carbon tetrafluoride makes it imperative to find solutions to destroy this potent greenhouse gas.

So far mostly catalytic and plasma discharge methods have been used to decompose $CF_4$.[1-3] Grytsinin et al. showed effective decomposition using a slipping surface discharge.[1] Whereas Takita et al. used $AlPO_4$-rare earth phosphate catalysts to decompose $CF_4$ at conversions of about 50 %.[2] Several papers like Jacobsohn et al. describe the decomposition as a means to deposit fluorinated amorphous-carbon films.[3]

In this research, we studied the effective decomposition of carbon tetrafluoride using microwave heating at medium power (0-1200 W) using water as a supplement and activated carbon as a catalyst. The experiments were carried out using an ASTEK microwave unit.

## Experimental

A simple setup was used as shown in Fig. 1. The feed is a mixture of carbon tetrafluoride, water (introduced by a bubbler), and nitrogen. The content of the feed gas is 4 % $CF_4$, 3 % water and balance nitrogen at a flow a rate of 15 mL/min. The active carbon (100 mg) was placed in a quartz tube and secured with quartz wool. This tube was then placed into the ASTEK microwave cavity (Fig 2.). The reaction mixture was continuously monitored with a MKS-UTI PPT quadrupole residual gas analyzer mass spectrometer with a Faraday cup detector and a variable high-pressure sampling manifold. The system was equilibrated at the beginning and then the power was turned on to the desired level and continued until an equilibrium value was achieved. The catalysts used were either prepared in our research group or used as obtained from commercial vendors.

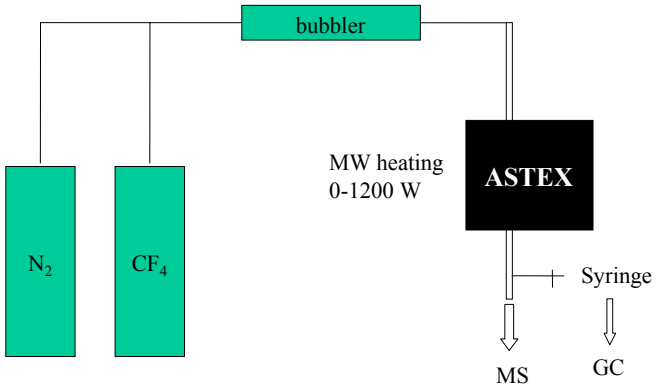


**Figure 1.** Schematic of the experimental setup for $CF_4$ decomposition.

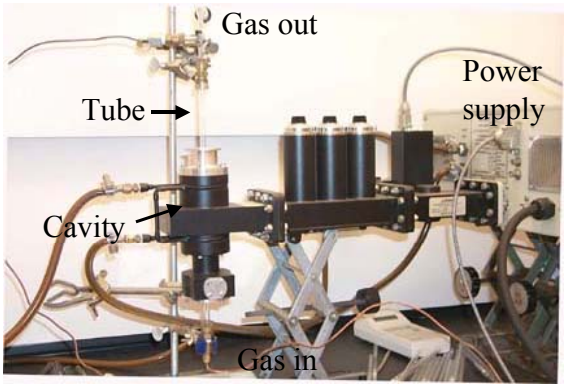


**Figure 2.** Photograph of the reaction setup

## Results and Discussion

Initial studies using discharge plasmas yielded only low conversions (up to 12 %). Additionally, MS studies suggest that $CF_4$ alone or $CF_4$ and water are the most suited systems. Studies using microwave heating exhibited promising results under similar conditions and were therefore pursued.

The reactions were carried out with the setup presented before at a constant flow rate of 15 mL/min. Several catalysts were tested in this line of experiments. The catalysts tested were several different kinds of activated carbon, Ni filament type catalyst, $V_2O_5$ Supported on $Al_2O_3$, and a zeolite/active carbon mixture.

Of these catalysts, only the activated carbon exhibited any change in the $CF_4$ concentration in these experiments. It was furthermore observed that no reaction takes place without the presence of water vapor.

In the case of activated carbon, several kinds of activated carbon were used, but the results presented here are the ones for a commercial brand available from Sigma-Aldrich. A typical decomposition versus time plot is shown in Fig. 3 as obtained with the mass spectrometer.

**Figure 3.** Plot of $CF_4$ decomposition versus time, top plot is the $CF_4$ plot, bottom plot is the $CO_2$ plot, power was turned on to 480 W (arrow= time of power on)

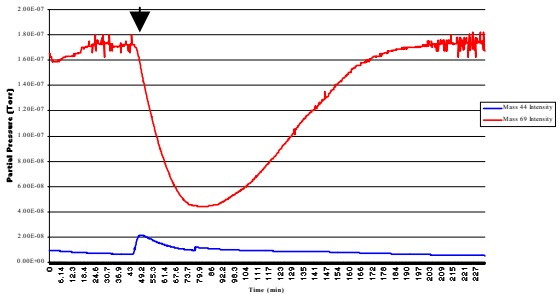

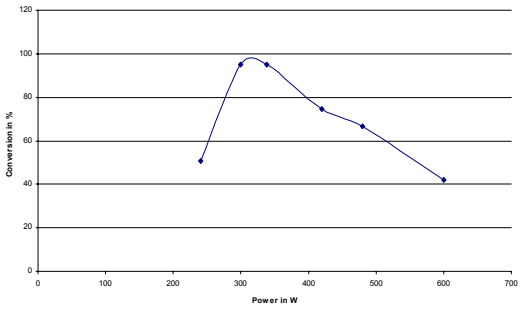


**Figure 4. Plot of Conversion of $CF_4$ versus Power in Watts**

The conversion was studied was a function of power. As shown in Fig. 4., the maximum conversion is achieved at medium power levels of 300-400 W (whole range 0-1200 W). The maximum conversion observed is 95 % measured as the disappearance of the $CF_4$ in the MS plot. As seen in the time versus conversion plot, the activated carbon deactivates rather quickly.

Furthermore, the reaction produces significant amounts of hydrogen, about 100,000 ppm. The extent of the reaction can also be seen on how the reaction tube looks after the reaction. The higher the extent of the reaction is, the more "decomposed" is the reaction tube due to the r\glow and HF production. The surface area of the activated carbon was determined to 653 $m^2/g$. It consists of meso- and micropores. The surface area below 20 Angstrom is 349 $m^2/g$, and between 20 and 200 Angstrom, it is 280 $m^2/g$.

The role of the water in this reaction is twofold. It is the primary energy absorber for the microwave radiation, but also it is the hydrogen and oxygen source needed in this reaction. It is believed that the carbon tetrafluoride reacts with the water under the use of the supplied microwave energy to yield hydrogen fluoride and carbon dioxide (The formed hydrogen fluoride is absorbed by a scrubber before it enters the mass spectrometer.). The reaction mechanism is believed to include the attack of hydrogen radicals on the $CF_4$ molecule; this is indicated by the formation of hydrogen in the reaction. Furthermore, the catalyst deactivation is thought to be due to the formation of hydrogen fluoride.

## Conclusions

The destruction of carbon tertrafluoride by microwave heating represents an efficient and easy means to get rid of this greenhouse gas. Carbon tetrafluoride is almost completely decomposed. The main products are hydrogen fluoride, carbon dioxide and hydrogen. The activated carbon catalyst deactivates after a short period of time. The deactivation time has to be prolonged. Furthermore it was found out that water is essential in these reaction and a reaction scheme was proposed.

**Acknowledgement.** The authors thank JFCC and Planet Japan for support of this research. We also thank Daniel Conde for assistance in the power measurements and reactor setup.

## References

(1) Grytsinin, S.I.; Korchagina, E.G.; Kossyi, I..A.; Misakyan, M.A.; Silakov, V.P.; Tarasov, N.M.; Temchin, S.M. *Plasma Sources Sci. Technol.* **10 (2001),** 125-133.

(2) Takita, Y.; Ninomiya, M.; Miyake, H.; Wakamatsu, H.; Yoshinaga, Y.; Ishihara, T. *Phys. Chem. Chem. Phys.* **1999, 1,** 4501-4504.

(3) Jacobsohn, L.G.; Franceschini, D.F.; Maia da Costa, M.E.H.; Freire Jr. F.L. *J. Vac. Sci. Technol. A* **18(5), Sept/Oct 2000,** 2230-2238.

synthesis and post-synthetic modification. When iron concentrations are kept low framework iron is seen (Fig 2).

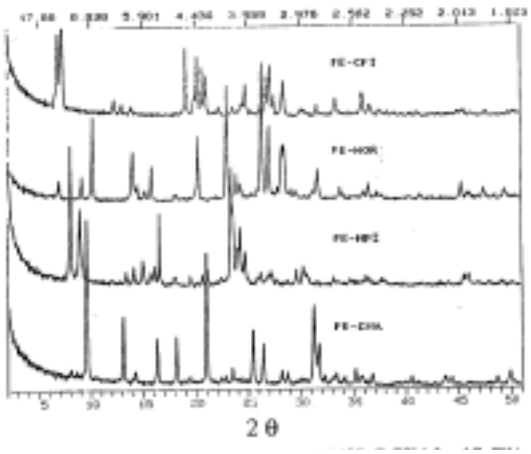


**Figure 2.** X-Ray Diffraction patterns of FeCIT-5, FeMOR, FeZSM-5 and FeCHA.

Extra-framework iron oxides are occluded after calcination of framework iron zeolites with high iron loading or physical mixtures of aluminum containing zeolites with iron salts or sublimation of iron by mixing zeolites with $Fe(acac)_2$ followed by an oxygen calcination procedure. The recent structure of CIT-5 is composed of 1D, extra-large pores of nearly circular cross section (center of O to center of O distance 9.91Å x 9.87Å) circumscribed by 14 T-atoms. The asymmetric unit contains 10 T-atoms and 19 oxygen atoms resulting in a unit cell content of $[Si_{32}O_{64}]$, a framework density of 18.3 T-atoms/1000 $Å^3$ and a density of 1.821 g/$cm^3$. The topology consists of zigzag ladders of 4-rings with pendant 5-rings interconnected through single zigzag chains. For CIT-5 (CFI) all structural parameters are within reasonable ranges for silicate materials ( d(Si-O) 1.591 Å with a range of 1.555-1.641 Å, a Si-O-Si angle of 149.4° with a range of 168.7°-140.6°, and an O-Si-O angle of 109.4° with a range of 113.8° - 104.2°. These values are appended to the molecular mechanics Universal Force Field (UFF) [3]. The UFF functional forms, parameters, and generating formulas for the full periodic table

**Table 1. Partial oxidation of methane with α-Fe sites in ZSM-5 and other Zeolites.**

| Zeolite | %wt Fe in | Oxidation | μmol Fe in sample | μmol. MeOH (oxygenate) |
|---|---|---|---|---|
| Fe-ZSM-5 Si/Al 11 | 0.5% | 5 Torr $N_2O$/ 250°C | 75 | - |
| Fe-ZSM-5 Si/Al 11 | 2.0% | 5 Torr $N_2O$/ 250°C | 360 | 97 |
| Fe-ZSM-5 Si/Al 11 | 5.0% | 5 Torr $N_2O$/ 250°C | 800 | 163 |
| Fe-ZSM-5 Si/Al 11 | 5.0% | 10Torr $N_2O$/250°C | 800 | 208 |
| Fe-CHA (0.1 μm) | 5.0% | 5 Torr $N_2O$/ 250°C | 800 | 10 |
| Fe-MOR (1-3 μm) | 5.0% | 5 Torr $N_2O$/ 250°C | 800 | 10 (33) |
| Fe-CIT-5 (3-7 μm) | 5.0% | 5 Torr $N_2O$/ 250°C | 800 | 4 (39) |

are used to model these structures. XRD, EXAFS, Mossbauer, DRS, magnetic measurements and EPR can resolve and attribute presence of lattice iron and extra-framework clusters. XRD for as made and calcined materials with iron in the lattice reveals α-$Fe_2O_3$ particles are absent ( no α-$Fe_2O_3$ reflection, $d_{104}$ = 2.70 Å). From EXAFS structural parameters obtained in the $k^3$ weighted optimization give 1.7, 2.7 and 3.4Å distances for $Fe^{(III)}$-oxygen, $Fe^{(III)}$- $Fe^{(III)}$ and $Fe^{(III)}$-Si bonds. In the EPR spectra the ratio of octahedral/tetrahedral iron can be assumed from the presence of lines at g= 2/4.3, and depends on sample hydration. In mononuclear iron complexes the Fe-O bond distances of 1.86 Å (2+, $O_h$) 6 coordinated and 1.90 Å (3+, $T_d$) 4 coordinated. For tetrahedral iron and silicon atoms bond distances of 1.65 for Si-O and 1.90 Å for Fe-O obtained from QM seen in the direction of the Fe-O-Si bridge, with Fe-O-Si angles close to the 131.2° and to a O-Fe-O angles of 109.47°.

**CONCLUSION**.

The reaction of the MMO binuclear heptapodate coordinated iron (III)-complexes of *N,N,N',N'*-tetrakis(iminomethyl)-2-hydroxy-1,3-diamino-propane model with methane is exothermic The σ- and π-bonds of the ferryl Fe=O in the plane of the Fe-O-Fe bridge, have the properties of a two atom three electron bond. After the H splitting from methane, the methyl recombines with the FeO center via a weak Fe-$OCH_3$ bond in this model.

Methane can also be converted into methanol with α-Oxygen at room temperature using $N_2O$ as a selective oxidant inside the pores of various zeolites. Extraction of the catalysts with water is preferred over acetonitrile-water mixtures. The dinuclear iron oxide clusters realize the sub-stoichiometric (based on a diiron sites) oxidation of methane after $N_2O$ activation, the small dinuclear Fe sites favor oxygen insertion chemistry over coupling chemistry.

**Acknowledgement.**

PPKG thanks ESA, FNRS and FSR Belgium for financial support, A.Fukuoka & M.Ichikawa from the CRC, at Hokkaido University, Sapporo, Japan for a collaboration on EXAFS. PPKG thanks WAGoddard III from the Material & Process Simulation Center, Beckman Institute (139-74), California Inst. of Technology, Pasadena CA, USA, WAG thanks BP Amoco for financial support.

**References**

(1) R.H. Crabtree, *Chem.Rev.*, **1995**, 95, 987.
(2) P.E. Siegbahn, R.H.Crabtree, *J.Am.Chem.Soc*., **1997**,*119*, 3103.
(3) P.P. Knops-Gerrits , P.A. Jacobs, A.Fukuoka, M.Ichikawa, F.Faglinoni, W.A. Goddard III, *J.Mol.Cat., A*, 166 (2001) 3, P.P. Knops-Gerrits, M. Witko, W.A.Goddard III, R. Millini Eds.
(4) K. Yoshizawa, K. Ohta, T. Yamabe, R. Hoffmann, *J. Am. Chem. Soc.*, **1997**, *119*, 12311.
(5) A.E.Shestakov, A.E.Shilov, *J.Mol.Cat., A*, 105 (1996) 1.
(6) A.K. Rappe, C.J. Casewit, K.S. Colwell, W.A. Goddard, W.M. Skiff, *J. Am. Chem. Soc.*, 114 (1992) 10024.; A.K. Rappe, W.A. Goddard, *J. Chem. Phys*., **1991**, 95, 3358.
(7) P.P. Knops-Gerrits, A.M. Van Bavel, G. Langouche, P.A. Jacobs, NATO ASI, **1998**, Derouane Eds., 3.44, 215.
(8) P.P. Knops-Gerrits, A. Verberckmoes, R.A. Schoonheydt, M. Ichikawa, P.A. Jacobs, *Micro- Mesop. Mat.*, **1998**, *21*: 4-6, 475.
(9) P.P. Knops-Gerrits, A. Weiss, S. Dick, P.A. Jacobs, *Stud.Surf.Sci.Catal*., **1997**, *110*, 1061.
(10) P.P. Knops-Gerrits, W.A. Goddard III, *J.Mol.Cat., A*, **2001**, 166, 1 & 135.
(11) Y. Oumi, M. Yamadaya, T. Kanougi, M. Kubo, A. Stirling, R. Vetrivel, E. Broclawik, A. Miyamoto, Catal. Lett., **1997**,45, 21.
(12) G.I., Panov, V.I., Sobolev, K.A. Dubkov,.A.E., Parmon, N.S., Ovanyesan, A.E., Shilov, A.A., Shteinman, *React. Kinet. Catal.Lett.*, **1997**, *61*, 251 .